Nano Energy 145 (2025) 111485

Contents lists available at ScienceDirect

Nano Energy

journal homepage: www.elsevier.com/locate/nanoen

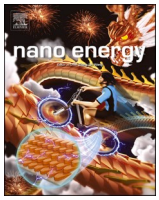

A versatile electrocatalytic [3+2] ring expansion approach for efficient electrosynthesis of oxa-/aza-heterocyclic compounds

Miao Wang [1], Zuoao Wu [1], Yulong Fu [1], Pengbo Zhang, Huaizhu Wang, Tianyu Shen, Qianchuan Yu, Xingkai Ma, Guochun Ding, Yizhi Xing, Zuoxiu Tie [*], Guoqiang Wang [*], Shuhua Li [*], Zhong Jin [*]

State Key Laboratory of Coordination Chemistry, MOE Key Laboratory of Mesoscopic Chemistry, MOE Key Laboratory of High Performance Polymer Materials and Technology, Jiangsu Key Laboratory of Advanced Organic Materials, Tianchang New Materials and Energy Technology Research Center, Institute of Green Chemistry and Engineering, School of Chemistry and Chemical Engineering, Nanjing University, Nanjing, Jiangsu 210023, PR China

ARTICLE INFO

Keywords:
Electrochemical ring enlargement
Electrodeposition of precious metal nanoparticles on carbon fibers
Lewis acid-mediated electrosynthetic processes
Cycloaddition route of epoxide scaffolds
C═O/C≡N bond activation and rearrangement

ABSTRACT

Electrosynthesis has emerged as a frontrunner in green chemistry, owing to its benign reaction conditions, high selectivity, tunable operating parameters, and eco-friendly features. Especially, the strategic synthesis of oxygen- and/or nitrogen-heterocyclic compounds holds great importance in across pharmaceutical, agrochemical, fragrance, polymeric, and clean energy sectors. Nevertheless, the electrochemical routes for crafting intricate heterocyclic compounds remain largely underexplored. Herein, we present an electrochemical [3 + 2] ring expansion approach that efficiently produces diverse O- and/or N-containing heterocyclic derivatives (e.g., 1,3-dioxolane, oxazoline, and cyclic carbonate) by fusing cheap and readily accessible precursors, e.g., acetone (CH_3COCH_3), acetonitrile (CH_3CN), or carbon dioxide (CO_2) with epoxide skeletons under ambient conditions. Experimental and computational investigations reveal the pivotal roles of cathodic noble metal nanocatalysts (e.g., Pt and Rh) deposited on carbon fibers and Lewis-acidic fluoroborate supporting electrolytes, promoting a kinetically favored concerted pathway over stepwise pathways in the electrocatalytic ring expansion cascade. Our analysis demonstrates that the differing activation energy barriers governing the crucial Lewis adduct [$2\pi + 2\sigma$]-cycloaddition step correlate with the higher reaction rate of acetone over acetonitrile, attributable to stronger electrostatic interactions observed in the acetone-participated reaction as elucidated by electrostatic potential surface analyses of transition states. This work underscores the prowess of electrochemical skeletal editing strategy in facilitating the green production of diversified heterocyclic organic compounds.

1. Introduction

Cyclic organic compounds, particularly heterocycles, play an important role in our society. For instance, over two-thirds of U.S. Food and Drug Administration (FDA) approved medicines incorporate N-heterocycle and/or O-heterocycle components [1–4]. The advancement of novel reaction routes to construct and manipulate ring structures is crucial in determining the properties and functionalities of organic molecules [5–8]. Previous studies have explored skeletal editing approaches through the introduction of carbon [9–13], nitrogen [14,15], oxygen [16], boron [17], or other species [18,19] into cyclic molecules. 1,3-Dioxolane, oxazoline and cyclic carbonate derivatives are versatile five-membered ring-containing molecules that find multifarious applications in various fields such as pharmaceuticals, biologics, pesticides, cosmetics, polymers, and clean energy industries. However, these compounds are typically synthesized via traditional thermochemical catalytic routes, and some of these methods are limited by harsh conditions, complex steps, low efficiency, large energy consumption, and the use of substantial amounts of catalysts [20–24]. Therefore, exploring an efficient ring expansion approach for synthesizing miscellaneous heterocyclic compounds by incorporating small molecules (such as acetone, acetonitrile or carbon dioxide) presents an intriguing alternative.

Electrochemical synthesis technique offers numerous advantages, including mild conditions, strong controllability, high efficiency, and the harnessing of economical electricity sourced from renewable

* Corresponding authors.
E-mail addresses: zxtie@nju.edu.cn (Z. Tie), wangguoqiang710@nju.edu.cn (G. Wang), shuhua@nju.edu.cn (S. Li), zhongjin@nju.edu.cn (Z. Jin).
[1] These authors contributed equally to this work

https://doi.org/10.1016/j.nanoen.2025.111485
Received 13 May 2025; Received in revised form 11 September 2025; Accepted 25 September 2025
Available online 26 September 2025

energies like solar and wind power [25–28]. These distinctive features have propelled the electrosynthesis methodology into the forefront of green synthetic chemistry, offering fascinating avenues for C–C functionalization, C–H activation, decarboxylative coupling, halogenation, borylation, metallo-organic coordination, and numerous other transformations. Nevertheless, efficient electricity-driven approaches for expanding rings to form oxygen- and/or nitrogen-containing heterocyclic organic compounds are seldom documented, and have consistently presented substantial challenges.

Herein, we report a versatile and scalable electrochemical [3 + 2] skeletal ring expansion strategy for the high-yield preparation of five-membered oxa-/aza-heterocycles (including 1,3-dioxolane, oxazoline, and cyclic carbonate) by inserting small molecules (e.g., acetone, acetonitrile, and carbon dioxide) into epoxide scaffolds, facilitated by the synergistic action of the cathodic metal electrocatalysts obtained via an *in situ* electrodeposition route on carbon fibers and a Lewis-acidic

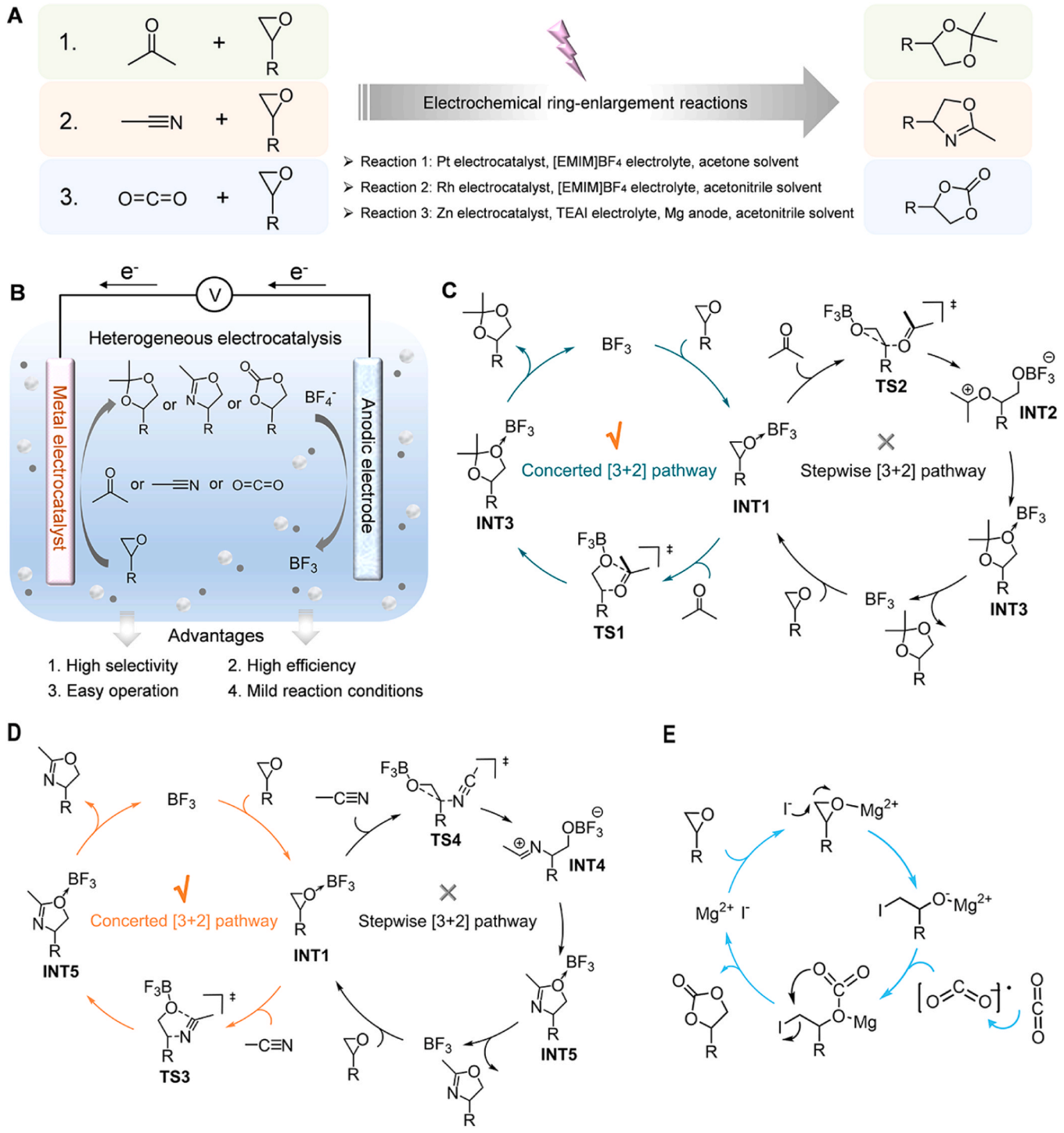

Fig. 1. The pathways, experimental configuration, and reaction routes of electrocatalytic ring expansion reactions. (A) Schematic reaction routes and (B) apparatus configuration of the electrochemical ring expansion approach for the synthesis of 1,3-dioxolane, oxazoline, and cyclic carbonate derivatives via the ring enlargement of epoxide scaffolds by small molecule units (e.g., CH_3COCH_3, CH_3CN, and CO_2). (C-E) Proposed and computed catalytic cycles of the BF_3-mediated coupling reaction pathways for the introduction of (C) CH_3COCH_3, (D) CH_3CN, and (E) CO_2 as insertion units into epoxide matrices.

fluoroborate mediator under ambient conditions. In this study, an electrically conductive carbon felt (CF) served as the substrate for nanocatalyst growth. Composed of interconnected carbon fibers, the CF's robust structure helps mitigate the detachment of electrocatalyst during electrochemical reactions. Additionally, the spatial confinement offered by the carbon fiber network helps prevent catalyst aggregation and surface oxidation, effectively preserving catalytic activity. Both experimental and computational analyses suggest that the proposed concerted ring expansion pathway is kinetically more favorable than the stepwise pathways in the electrochemical reactions. The reaction rate of acetone ($\sim$95 mmol h^{-1} $cm_{cat.}^{-2}$) surpasses that of acetonitrile ($\sim$39 mmol h^{-1} $cm_{cat.}^{-2}$) due to the difference in activation energy barrier for the rate-determining step of Lewis adduct [2π+ 2σ]-cycloaddition process. Furthermore, the efficient electrochemical synthesis of cyclic carbonates has also been accomplished through the utilization of the greenhouse gas CO_2 molecule as the pivotal insertion unit, underscoring its immense potential for facilitating carbon neutralization efforts. This study exemplifies the practicality of electrochemical skeletal editing strategies in achieving eco-friendly green synthesis of diversiform heterocyclic organic products.

2. Results and discussion

2.1. Electrochemical ring expansion strategy and electrocatalytic reaction pathways

Value-added oxa-/aza-heterocycle molecules, such as five-membered 1,3-dioxolane, oxazoline, and cyclic carbonate derivatives, frequently serve as key building blocks, ligands, or chelating agents in the synthesis of more complicated organic and organometallic compounds. Nevertheless, the conventional thermochemical methods to produce these molecules are intricate, and the raw materials involved are economically burdensome. Global production statistics reveal a substantial annual output of approximately ~15,000,000 tons of acetone (CH_3COCH_3) and ~3,400,000 tons of acetonitrile (CH_3CN) in 2022. Alarmingly, global emissions of the industrial exhaust gas, carbon dioxide (CO_2), have surpassed a staggering 36.8 gigatons in 2022, exacerbating the global climate change. The strategic harnessing of CH_3COCH_3, CH_3CN, and CO_2 as cost-effective and abundant raw materials in organic synthesis holds immense intrigue, promising significant economic gains and industrial significance. To achieve this objective, we introduce an electrochemical ring expansion methodology that proficiently enlarges three-membered epoxides through the insertion of these characteristic C═O/C≡N-bearing molecules, enabling the highly selective synthesis of 1,3-dioxolane, oxazoline, and cyclic carbonate derivatives, as schematically depicted in Fig. 1A-1B. Electrochemical organic synthesis offers several key advantages over traditional thermal catalysis route, including mild conditions, high selectivity, and low energy consumption (direct electron transfer avoids high temperature and hazardous reagents). It also has a minimal environmental footprint, as it can make use of renewable electricity and generates less waste, making it a greener and more sustainable alternative for chemical manufacturing. This innovative process employs cathodic metal/alloy electrocatalysts and fluoroborate-containing ionic liquid supporting electrolytes, as detailed in the Experimental section of Supplementary Materials. This BF_3 source originated from fluoroborate-containing ionic liquid has many merits as follows: (1) The *in-situ* generation process through simple galvanostatic electrolysis eliminates the need for storage procedures; (2) It allows for easy dosing by turning the current on and off; (3) The process produces no harmful fumes due to strong interaction with the ionic liquid; (4) It exhibits low sensitivity to moisture, as the ionic liquid protects against humidity.

Fig. 1C illustrates the electrocatalytic cycle for the ring expansion reaction of aromatic epoxides exemplified by styrene oxide, utilizing acetone as the insertion moiety. Initially, the complexation of styrene oxide with BF_3 species originated from fluoroborate-based ionic liquid forms the Lewis adduct **INT1**, which is exothermic by 4.3 kcal mol^1. Then, the **INT1** reacts with acetone through either a concerted mechanism (cyan line, via transition state 1, namely **TS1**) or a stepwise mechanism (black line, starting with a BF_3-mediated ring-opening reaction of styrene oxide via transition state 2, namely **TS2**) to yield the intermediate products. Computational analyses reveal that the concerted ring expansion reaction pathway exhibits kinetic superiority over the stepwise pathway, and the detailed discussion of this kinetic preference is provided in subsequent sections. Additionally, Fig. 1D and Fig. 1E depict the electrocatalytic cycles for ring expansion reactions featuring the insertion of acetonitrile and carbon dioxide molecules, respectively. In the former scenario, the BF_3-bearing ionic liquid plays a pivotal role as a reaction mediator, whereas in the latter, the sacrificial magnesium metal anode functions as a Lewis acidic electrocatalyst, efficiently promoting the targeted ring expansion reactions.

2.2. Electrochemical ring expansion of epoxides by reacting with acetone

The electrochemical ring expansion reaction route of styrene oxide (**1a**) with acetone for the synthesis of 2,2-dimethyl-4-phenyl-1,3-dioxolane (**1b**) was carried out using a standard three-electrode system in an undivided electrochemical cell at room temperature (Fig. 2). Typically, the working electrode (i.e., cathode) was a piece of carbon felt (CF, 1 × 1 cm^2) electrodeposited with platinum nanoparticles (namely Pt-NPs/CF), while a graphite rod and a standard Ag/AgCl electrode were used as the counter electrode (i.e., anode) and reference electrode, respectively (Fig. 2A). Under a constant current density of 20 mA/cm^2, the output voltage for the electrochemical ring expansion reaction producing **1b** is approximately −1.4 V (*vs.* Ag/AgCl). To investigate the influence of electrocatalysts on the results of electrosynthesis, we further prepared and compared a range of other cathodic electrocatalysts by loaded with various metal/alloy nanoparticles (Fig. S1). These included unary metals such as Pt, Rh, Pd, Au, and Ru, binary alloys comprising AuPt and RuPt, and a ternary alloy consisting of RhRuPt. As shown in Fig. 2B-2C and Fig. S2-S13, the crystalline structures, morphological features and chemical compositions of the as-prepared electrocatalysts were comprehensively characterized, verifying their successful preparation [29–31]. The resultant cathodic electrocatalysts display a 3D-crosslinked scaffold distinguished by a uniform distribution of particles and a plethora of exposed active sites. These attributes facilitate efficient mass transport and enhance the adsorption and desorption processes of reaction intermediates. The electrocatalytic stability of Pt-NPs/CF electrode was evaluated through cycling tests, as depicted in Fig. 2D. After five cycles, the yield remained at approximately 90 %. The screening experiments were performed utilizing the prepared cathodic electrocatalysts. As illustrated in Fig. S14, the yields of **1b** obtained from these cathodic electrocatalysts underscore the exceptional performance of the Pt-NPs/CF cathode, which attained a yield of approximately 95 % after a reaction duration of 1 h along with a **1b** reaction rate of ~95 mmol h^{-1} $cm_{cat.}^{-2}$. The voltage–time (V-t) profiles under different applied current densities and supporting electrolyte concentrations are presented in Fig. S15 and Fig. S16, respectively. When a current density of −10 mA cm^{-2} and a supporting electrolyte concentration of 0.05 M were applied, reactant signals remained detectable via GC-MS within the 1-hour reaction period. In contrast, under conditions of −50 mA cm^{-2} and 0.2 M supporting electrolyte, a noticeable decline in energy efficiency (EE) accompanied by a rise in reaction cost that is undesirable from both economic and energetic standpoints.

The impact of various ionic liquid supporting electrolytes, featuring different molecular structures and compositions, on the yield of **1b** was also explored (Fig. S17 and Fig. 2E). Among the fluoroborate-containing ionic liquids, 1-ethyl-3-methylimidazolium tetrafluoroborate ([EMIM]BF_4) demonstrated the highest yield of **1b** when associated with the Pt-NPs/CF cathode. Notably, supporting electrolytes devoid of fluoroborate ions, such as tetraethylammonium bromide (TEAB) and tetraethylammonium iodide (TEAI), exhibited negligible yields of product **1b**.

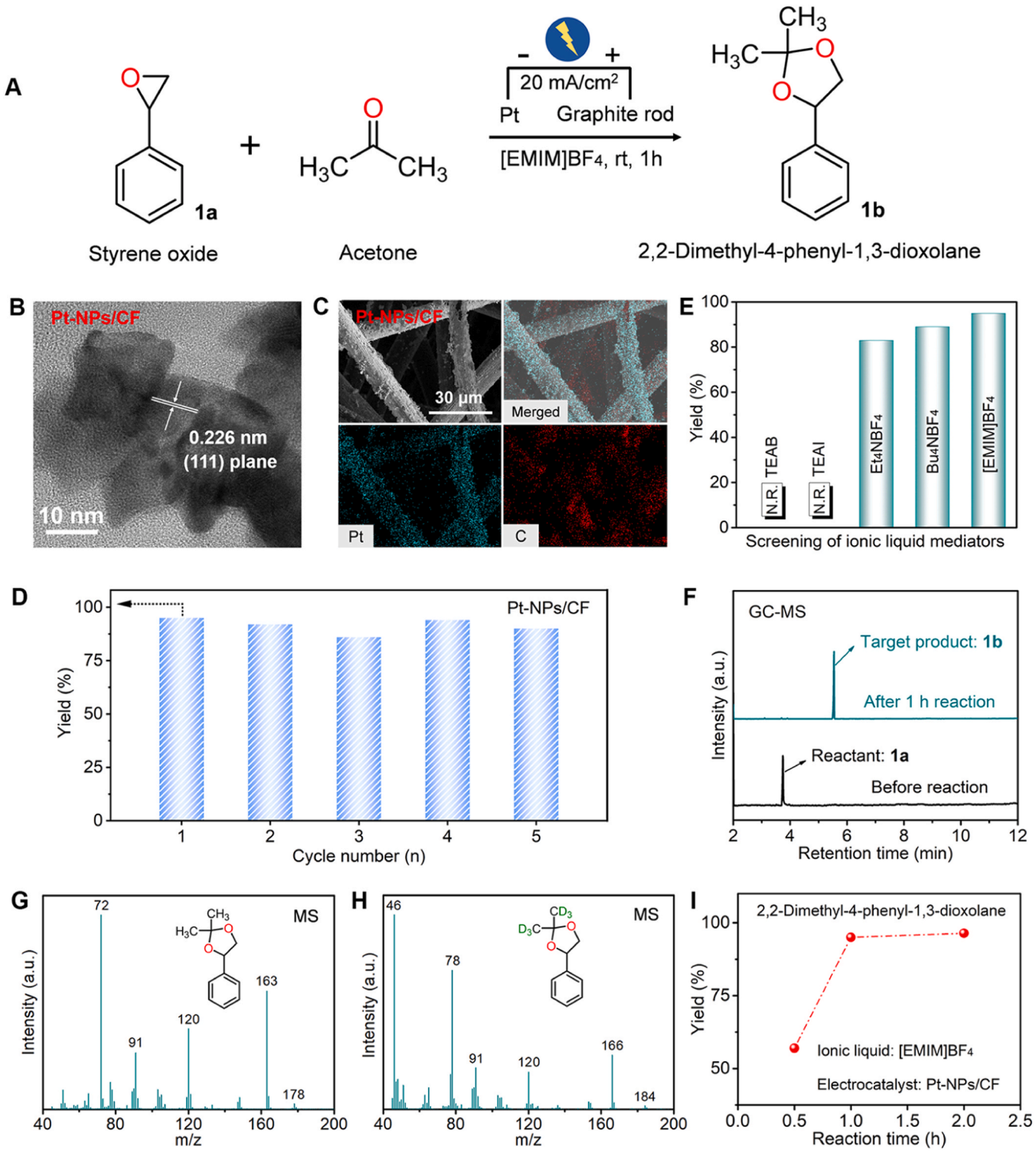

Fig. 2. Electrochemical ring expansion of epoxides by reacting with acetone. (**A**) Electrocatalytic cycloaddition route of styrene oxide (**1a**) with acetone to produce 2,2-dimethyl-4-phenyl-1,3-dioxolane (**1b**). Typical reaction conditions: styrene oxide (**1a**, 100 mM), acetone (30 mL), supporting electrolyte ([EMIM]BF_4, 100 mM), Pt-NPs/CF cathode, and graphite rod anode in an undivided electrolytic cell under a constant current density of 20 mA/cm^2 for 1 h at room temperature. (**B**) HRTEM image and (**C**) SEM and corresponding elemental mapping images of Pt-NPs/CF electrocatalyst. (**D**) Cycling tests of Pt-NPs/CF cathode for the **1b** production. (**E**) The yields of **1b** using various ionic liquid supporting electrolytes; N.R. = no reaction. (**F**) GC-MS analyses before and after 1 h of electrochemical ring expansion reaction with Pt-NPs/CF electrocatalyst and [EMIM]BF_4 supporting electrolyte. (**G**, **H**) MS plots of the product **1b** derived from (**G**) acetone and (**H**) deuterated acetone, respectively. (**I**) The accumulative yield of **1b** within the reaction duration of 2 h.

These findings emphasize the pivotal role of Lewis-acidic BF_3-containing ionic liquids as crucial mediators and electron acceptors in the electrochemical ring expansion process. Conversely, the halogen ions present in TEAB and TEAI predominantly function as Lewis basic "electron pair donor" and nucleophile, thus lacking of the superior attributes of Lewis-acidic electrocatalysts.

Qualitative analyses of product **1b** were performed using gas chromatography-mass spectrometry (GC-MS) by utilizing the Pt-NPs/CF cathodic electrocatalyst and $[EMIM]BF_4$ supporting electrolyte under the optimized reaction conditions. The GC-MS results in Fig. 2F revealed

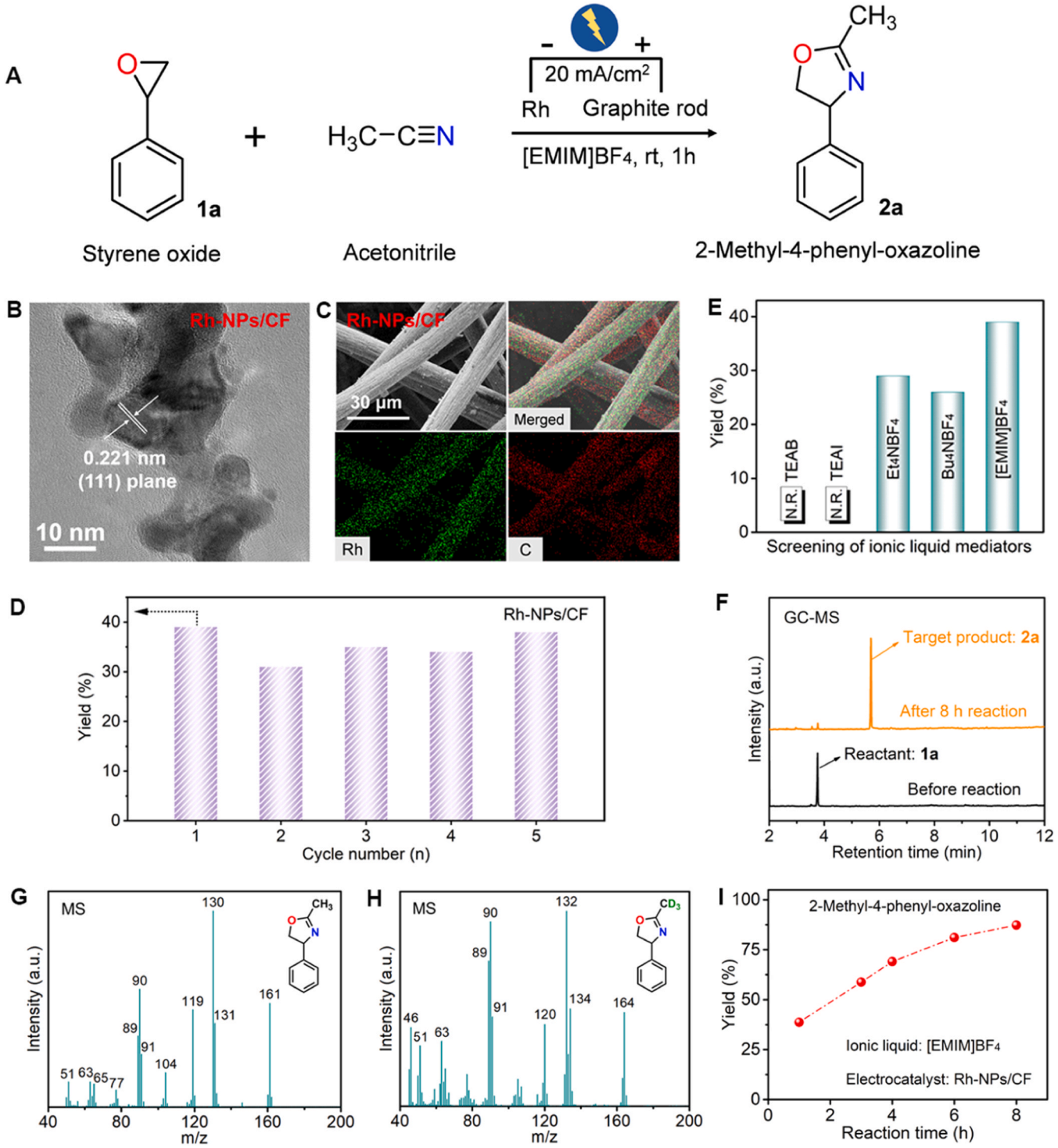

Fig. 3. Electrochemical ring expansion of epoxides by reacting with acetonitrile. (**A**) Electrocatalytic cycloaddition route of styrene oxide (**1a**) with acetonitrile to produce 2-methyl-4-phenyl-oxazoline (**2a**). Typical reaction conditions: styrene oxide (**1a**, 100 mM), acetonitrile (30 mL), supporting electrolyte ($[EMIM]BF_4$, 100 mM), Rh-NPs/CF cathode, and graphite rod anode in an undivided electrolytic cell under a constant current density of 20 mA/cm^2 for 1 h at room temperature. (**B**) HRTEM image and (**C**) SEM and corresponding elemental mapping images of Rh-NPs/CF electrocatalyst. (**D**) Cycling tests of Rh-NPs/CF cathode for the **2a** production. (**E**) The yields of **2a** using various ionic liquid supporting electrolytes; N.R. = no reaction. (**F**) GC-MS analyses before and after 8 h of electrochemical ring expansion reaction with Rh-NPs/CF electrocatalyst and $[EMIM]BF_4$ supporting electrolyte. (**G**, **H**) MS plots of the product **2a** derived from (**G**) acetonitrile and (**H**) deuterated acetonitrile, respectively. (**I**) The accumulative yield of **2a** within the reaction duration of 8 h.

that the characteristic peak of reactant **1a** appeared at a retention time of 3.75 min was completely consumed after 1 h of electrochemical reaction, resulting in a superior selectivity towards the formation of target product **1b**, which shows a strong peak at the retention time of 5.53 min, with no detectable byproducts present. The peak in MS plots appears at $m/z = 178$, representing the intact molecular ion (M^+) for **1b** without fragmentation. A peak at $m/z = 163$ can be observed, which is originated from the loss of a methyl group (-CH_3) from the molecular ion peak. Another notable peak at $m/z = 91$ signifies a stable aromatic ion associated with the loss of the dioxolane moiety, resulting in a toluene-like structure (Fig. 2G). Furthermore, a deuterium isotope labeling experiment was conducted using deuterated acetone (CD_3COCD_3) reagent, demonstrating MS peak shifts that clearly indicated the successful incorporation of deuterated acetone into product **1b**, as shown in Fig. 2H. Subsequently, the high purity of the isolated product **1b** was further verified through ^1H and ^{13}C nuclear magnetic resonance (NMR) spectroscopies (Fig. S18-S19). The time-dependent yield of **1b** was also assessed (Fig. 2I). The results exhibited a swift increase in product quantity and ultimately achieved a plateau yield of approximately 95 % after 1 h, indicating a relatively high reaction rate and an efficient reagent conversion ratio.

Electrochemical impedance spectroscopy (EIS) measurements revealed distinct charge transfer characteristics between the cathodic electrocatalysts, as displayed in Fig. S20. The Nyquist plots showed that Pt-NPs/CF exhibited a reduced charge transfer resistance (Rct), suggesting enhanced electron mobility within the electrode interface. Structural characterizations of Pt-NPs/CF electrode were performed before and after the cycling tests using multiple analytical techniques (Fig. S21-S23).

Furthermore, we developed a decagram-scale synthesis protocol for the electrocatalytic dioxolanation reaction by utilizing low-cost graphite rod and platinum plate electrodes in an undivided electrochemical cell under constant current conditions. These mild and operationally simple setups offered opportunities for large-scale electrosynthetic applications. By increasing both substrate concentration and electrode surface area, the dioxolanation reaction of styrene oxide was efficiently scaled up, yielding the target product in approximately 86 % (15.3 g) (Fig. S24). This result demonstrates that this electrochemical strategy created a practical route to high-value-added chemicals.

2.3. Electrochemical ring expansion of epoxides by reacting with acetonitrile

For comparison, Fig. 3A delineates the reaction pathway for the ring expansion of **1a** with acetonitrile, leading to the formation of 2-methyl-4-phenyl-oxazoline (**2a**). The output voltage of ring-enlargement reaction for the electrosynthesis of **2a** is around −1.2 V (*vs.* Ag/AgCl) at a fixed current density of 20 mA/cm^2. The cycling tests of Rh-NPs/CF electrocatalyst for the **2a** production is shown in Fig. 3D. Screening experiments were conducted to assess the yields of **2a** using diverse cathodic electrocatalysts (Fig. S25) and supporting electrolytes (Fig. 3E). The results indicated that the Rh-NPs/CF cathode combined with the [EMIM]BF_4 electrolyte exhibited the highest yield after a reaction duration of 1 h with a **2a** reaction rate of ~39 mmol h^{-1} $cm_{cat.}^{-2}$. The superior electrocatalytic performance of the Rh-NPs/CF cathodic electrocatalyst is primarily ascribed to its favorable electronic structure and robust capacity for reactant adsorption. The d-orbitals of the rhodium metal enable optimal interactions with the substrates, thereby facilitating efficient activation and weakening of the reactant bonds [10,12].

Meanwhile, the supporting electrolyte containing BF_4^- anions demonstrated superior performance as a crucial Lewis-acidic mediator in the electrochemical ring expansion process (Fig. 3E). This attribute is particularly pivotal, as bond activation is indispensable for the ring-opening of epoxides. To delve deeper into the influence of BF_4^- anions, cyclic voltammetry (CV) experiments were conducted from −3.5 V to 3.5 V (*vs.* Ag/AgCl) using a pristine CF cathode in either TEAB or [EMIM]BF_4 supporting electrolytes. In the presence of [EMIM]BF_4, distinct redox peaks emerged, clearly indicating the occurrence of the desired electrochemical coupling reaction (Fig. S26). Conversely, when using the fluoroborate-free TEAB supporting electrolyte, the signal corresponding to **2a** was absent, aligning with the previous discussion on the synthesis of **1b**.

Gas chromatography-mass spectrometry (GC-MS) and high-performance liquid chromatography (HPLC) analyses were conducted to evaluate the production of target product **2a** before and after an 8-h reaction period (Fig. 3F and Fig. S27), confirming the high selectivity for **2a** production which has a retention time of 5.71 min in GC-MS and 4.62 min in HPLC, respectively. The molecular ion peak (M^+) in MS results appears at $m/z = 161$, which corresponds to the intact molecule of **2a**. A fragmentation pathway may involve the loss of a hydrogen atom, leading to the peak around $m/z = 160$. Further fragmentation may involve the cleavage of a methyl group and a phenyl moiety, or the rearrangement of the aromatic system, leading to the formation of a fragment ion at $m/z = 104$. Moreover, the heterocyclic ring could undergo a ring opening process, generating fragment ions at m/z value such as 89 or lower. These fragments may arise from the loss of neutral species (such as -NH or other small fragments), as displayed in Fig. 3G. In a deuterium isotope labeling experiment, the MS plot exhibited clear shifts in peaks from $m/z = 131$–134 and $m/z = 161$–164, indicating successful incorporation of deuterated acetonitrile (CD_3CN) onto **1a** (Fig. 3H). Furthermore, the Fourier-transform infrared (FTIR) spectra of the liquid product revealed specific coordination environments, featuring a peak around 1677 cm^{-1} originated from the C═N bond of **2a** (Fig. S28). The ^1H NMR and ^{13}C NMR analyses for the isolated product **2a** were presented in Fig. S29 and Fig. S30, respectively, further confirming its high purity. Under optimal reaction conditions utilizing the Rh-NPs/CF cathodic electrocatalyst and [EMIM]BF_4 supporting electrolyte, the cumulative yield of **2a** progressively increased with prolonged reaction time, ultimately reaching approximately 87 % after an 8-h reaction (Fig. 3I). The electrocatalytic ring-expansion route developed in this study for the synthesis of value-added 1,3-dioxolane and oxazoline compounds is compared with representative thermo-catalytic and photo-catalytic approaches from the literature in Table S1, which demonstrates that our electrochemical strategy achieves a very competitive reaction efficiency under milder conditions.

2.4. Expandability for the synthesis of diverse 1,3-dioxolane and oxazoline derivatives

To assess the expandability of fluoroborate-mediated [3 + 2] electrochemical ring expansion approach, we investigated the versatility of this protocol across a range of substituted epoxide substrates (Fig. 4A). We are particularly focused on halogen-substituted substrates, which are of great significance in the pharmaceutical industry and drug discovery [32,33]. Fig. 4B depicts the isolated yields for 1,3-dioxolane derivatives, with halogen-containing products yielding between 71 % and 80 %, while the methylated product (**1m**) yielded approximately 67 % after a reaction duration of 1 h. Analogously, extension experiments were conducted to synthesize oxazoline-based derivatives, achieving isolated yields for the halogenated products ranging from 66 % to 74 %, while the methylated product (**2g**) yielded approximately 62 % after a reaction time of 8 h, as shown in Fig. 4C. The MS analysis results for all target compounds are provided in Fig. S31–S41. Broadly, the yield percentages of 1,3-dioxolane derivatives were higher than those of oxazoline derivatives. This difference is potentially attributable to variations in the energy barriers of the respective reactions, which will be elaborated in subsequent mechanistic investigations.

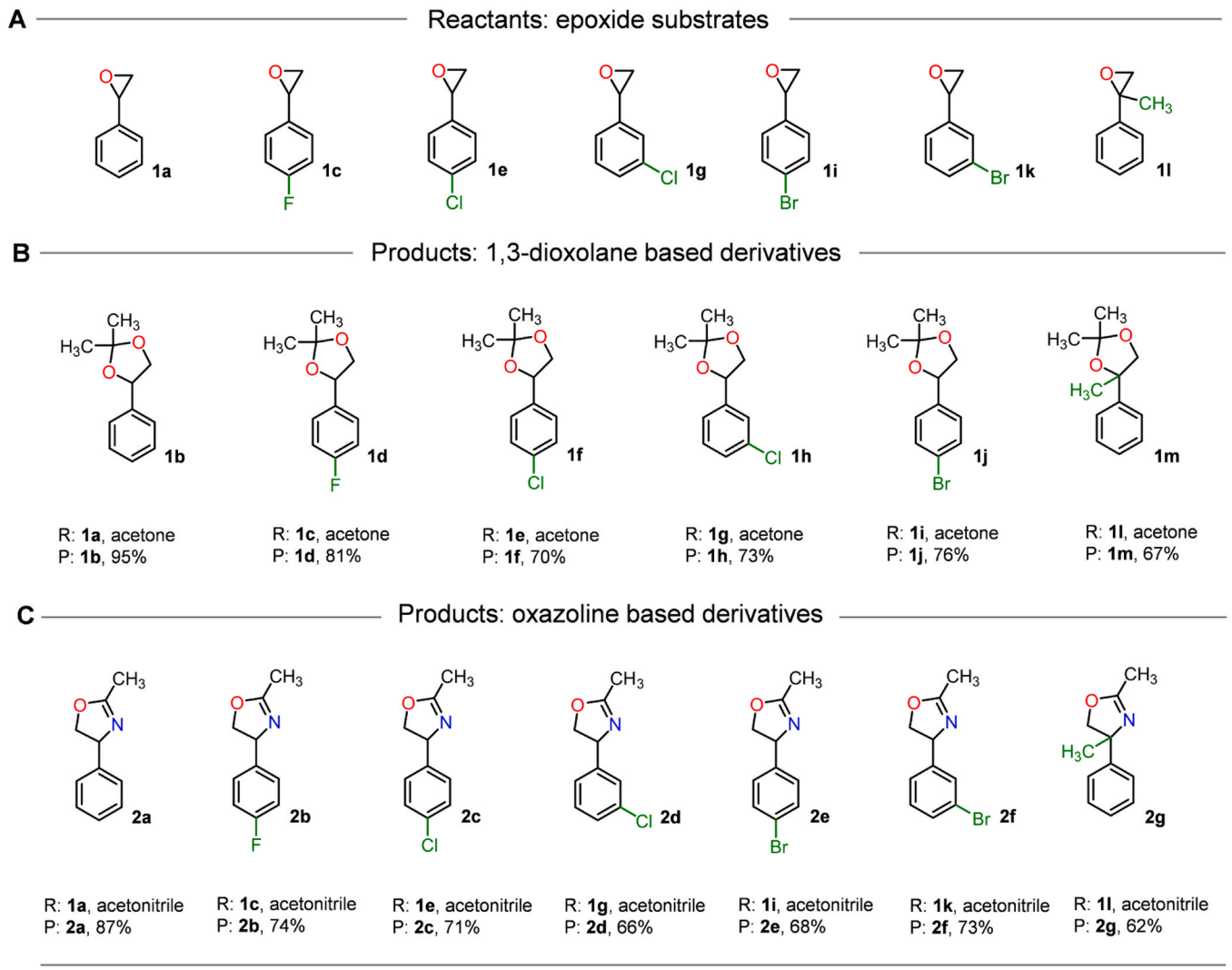

Fig. 4. Substrate universality for electrochemical ring expansion of (**A**) aromatic epoxides reacted with (**B**) acetone and (**C**) acetonitrile precursors for the synthesis of 1,3-dioxolane and oxazoline derivatives; "R" and "P" correspond to reactant and product, respectively.

2.5. Electrochemical ring expansion of epoxides by reacting with carbon dioxide

To achieve a carbon-neutral cycle, considerable research has been dedicated to developing efficient coupling reactions that convert greenhouse gas CO_2 feedstock into economically viable products [34–40]. One promising approach, characterized by high atomic economy, involves the conversion of CO_2 and epoxides into cyclic carbonates, which are valuable for producing polycarbonates and as polar aprotic solvents in batteries. Traditionally, the synthesis of cyclic carbonates has involved the addition of CO_2 to epoxides, facilitated by metal halides or complexes as catalysts, under conditions of high pressure and temperature [41]. In this study, we propose the electrochemical ring expansion route as a greener and more energy-efficient alternative for the preparation of cyclic carbonates.

The typical reaction conditions to facilitate the electrochemical ring-opening reaction of **1a** for producing styrene carbonate (**3a**) under atmospheric CO_2 pressure and ambient temperature are outlined in Fig. S42A. This carboxylation process is promoted by the synergistic effect of tetraethylammonium iodide (TEAI) ionic liquid supporting electrolyte as an ionic liquid supporting electrolyte and electrogenerated Mg^{2+} salt derived from sacrificial Mg anode as a Lewis acidic mediator. Moreover, the effects of various cathodic electrocatalysts and supporting electrolytes on the yield of **3a** were also investigated, as illustrated in Fig. S42B and Fig. S42C, respectively. The XRD patterns of all metal electrodes and the Zn 2p XPS result for Zn foil are depicted in Fig. S43 and Fig. S44, respectively. The results show that the zinc (Zn) foil cathode and TEAI supporting electrolyte exhibit superior performance for the **3a** production. The d-electrons of cathodic Zn electrocatalyst contribute to its ability for stabilizing intermediate species or transition states during this reaction, thereby facilitating electron transfer and lowering activation energy. Moreover, Zn is known for its low cost, abundance, and environmental friendliness compared to other precious metals, making it an attractive option for practical industrial applications. The yield of **3a** using TEAI as a supporting electrolyte is higher than that using TEAB, which is attributed to the stronger nucleophilicity of I^- compared to Br^-. As a nucleophilic reagent, I^- can effectively attack the C-O bonds of epoxides, facilitating the opening of the oxygen-containing three-membered rings and leading to the formation of the key intermediate that ultimately produces the pentacyclic carbonates. In contrast, BF_4^-, essential in the electrochemical synthesis of 1,3-dioxolane and oxazoline derivatives, lacks nucleophilicity and does not possess the reactivity required to generate cyclic carbonate products. The mass spectrum (MS) result for the target product (**3a**) is depicted in Fig. S42D. The molecular ion peak (M^+) at $m/z = 164$ corresponds to the intact molecule of **3a**. A potential fragmentation pathway involves the loss of carbon dioxide, forming a fragment ion at $m/z = 120$. Additional fragment ions are possibly derived from the aromatic system. For instance,

the peak at $m/z = 91$ can be attributed to a stable benzyl cation fragment, while $m/z = 77$ may arise from other aromatic rearrangements.

2.6. Theoretical simulations and reaction mechanism studies

To gain mechanistic insight into the ring expansion reactions of epoxide precursors, density functional theory (DFT) calculations were conducted using the M06–2X functional with acetone and acetonitrile as the model molecules, as depicted in Fig. 5 [42–45]. Previous research by Feroci's group reported that the *in-situ* formation of BF_3 through the direct anodic oxidation of fluoroborate-containing ionic liquid has the potential to enhance reaction yields in organic synthesis [46]. Our investigation revealed that when employing various ionic liquid supporting electrolytes, only those with BF_4^- as the counter anion could

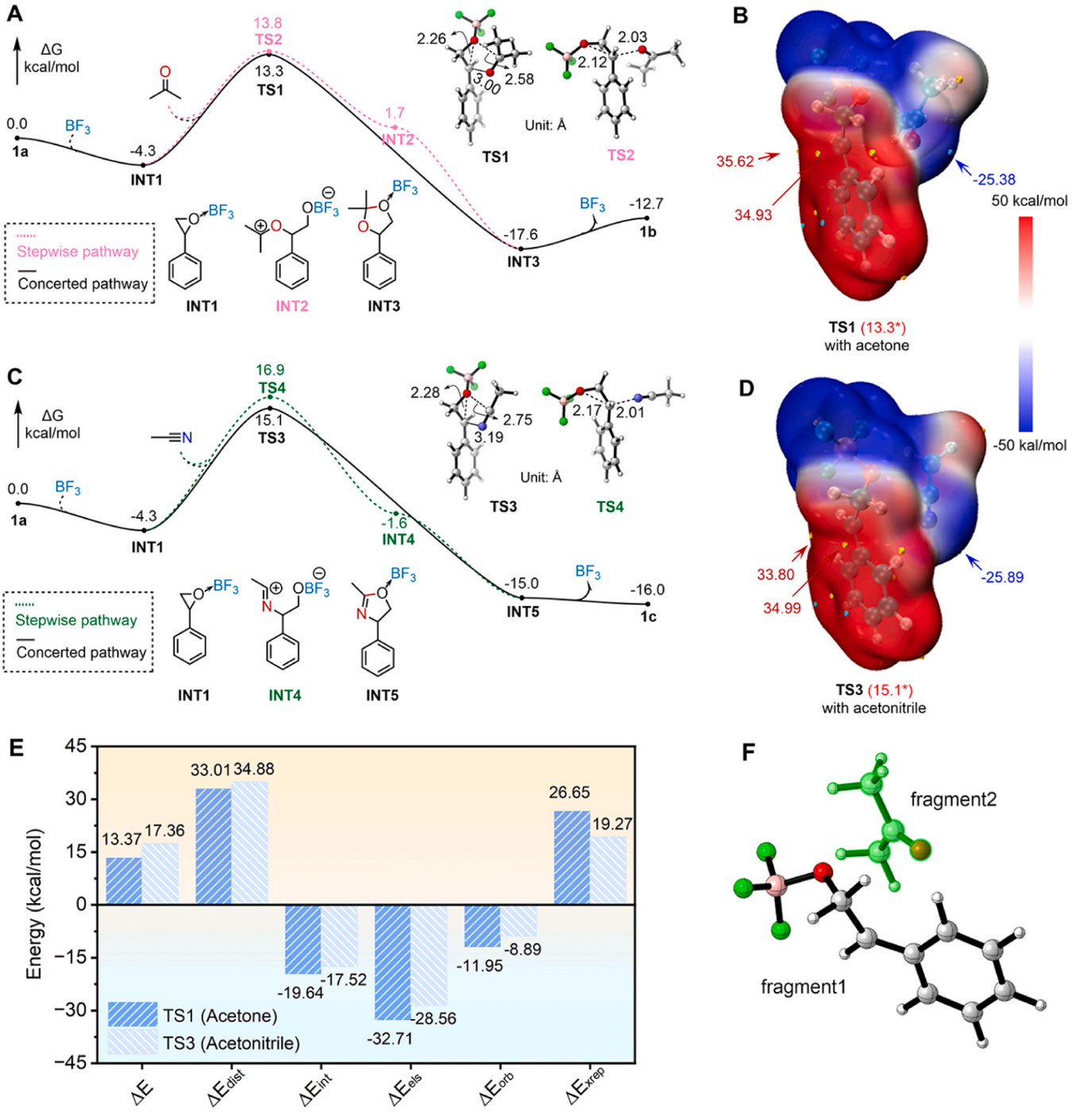

Fig. 5. Theoretical calculations on the possible electrochemical ring expansion reaction pathways of epoxides. (**A**, **C**) The computed Gibbs free energy profiles for the different pathways in electrochemical ring expansion reaction of **1a** with (**A**) acetone and (**C**) acetonitrile (in kcal mol^{-1}). The unit of distances is in Å. (**B**, **D**) The electrostatic potential surfaces of two electrochemical ring expansion transition states: (**B**) **TS1** with acetone and (**D**) **TS3** with acetonitrile (in kcal mol^{-1}). The positions pointed by the arrows correspond to the extreme points of the electrostatic potentials on the reaction site surfaces (blue arrow indicates the negative potential that attracts positive charge; red arrow indicates the positive potential that attracts negative charge). (E) Comparison of the energy components of transition states **TS1** and **TS3** via energy decomposition analysis (EDA). This analysis reveals the contributing factors (distortion, electrostatic, and orbital interactions) to the overall activation barrier difference between the acetone and acetonitrile pathways. (F) The fragmentation model for **TS1**.

initiate the ring-enlargement processes of epoxide substrates under a negative bias. The BF_4^- containing ionic liquids serve as both a supporting electrolyte and a crucial mediator. In this work, the HPLC chromatogram collected during the electrochemical ring expansion reaction (Fig. S45) provides direct evidence for the *in-situ* generation of BF_3 intermediate. The *in-situ*-formed BF_3 intermediate, acting as a Lewis acid electrocatalyst, can effectively weaken the C–O bond of epoxide group and lower the activation energy of the rate-determining step in the subsequent epoxide cleavage process [20,24].

As illustrated in Fig. 5A, the acetone-mediated reaction commences with the coordination of BF_3 to the epoxide **1a**, forming the intermediate **INT1** ($\Delta G = -4.3$ kcal/mol). From **INT1**, two competing pathways for the nucleophilic attack of acetone were identified: a concerted pathway (solid black line) and a stepwise pathway (dashed pink line). The concerted pathway proceeds via transition state **TS1**, representing the rate-determining step with a Gibbs free energy barrier of 13.3 kcal/mol. The alternative stepwise pathway, via **TS2** and the intermediate **INT2**, faces a slightly higher barrier of 13.8 kcal/mol. Given the low barrier difference (within 0.5 kcal/mol), though the concerted pathway is lower in energy, both pathways are kinetically accessible. The corresponding reaction profile for acetonitrile is depicted in Fig. 5C. The reaction follows a similar mechanistic scenario, with the concerted pathway (**TS3**, $\Delta G^{\ddagger} = 15.1$ kcal/mol) being kinetically favored over the stepwise pathway (**TS4**, $\Delta G^{\ddagger} = 16.9$ kcal/mol). Compared with acetone, the reaction of acetonitrile requires much higher barrier height ($\Delta\Delta G^{\ddagger} = 1.8$ kcal/mol). From a qualitative perspective, these results explain the observed slower reaction rate of acetonitrile ($\sim$39 mmol h^{-1} $cm_{cat.}^{-2}$) compared to acetone ($\sim$95 mmol h^{-1} $cm_{cat.}^{-2}$), attributed to a kinetical effect.

To uncover the physical origins of this kinetic preference, we analyzed the electronic and structural properties of the related cyclization transition states, **TS1** and **TS3** [47–49]. The electrostatic potential (ESP) maps rendered on the van der Waals surfaces of these transition states (Fig. 5**B**) provide the insight that, in **TS1**, there is a strong electrostatic complementarity between the electron-rich carbonyl oxygen of acetone ($V = -25.4$ kcal/mol) and the highly electron-deficient, electrophilic carbon of the BF_3-activated epoxide ($V = 35.6$ kcal/mol). While **TS3** displays a similar interaction, the positive potential on the corresponding electrophilic carbon is less intense ($V = 33.8$ kcal/mol), suggesting a weaker electrostatic driving force (Fig. 5D). This qualitative picture could be further quantified by energy decomposition analysis (EDA) [50], with the results for **TS1** and **TS3** compared in Fig. 5E-5F. The analysis partitions the activation strain energy ($\Delta E^{\ddagger}$) into the energy required to distort the reactants into their TS geometry ($\Delta E_{dist}^{\ddagger}$) and the interaction energy between them ($\Delta E_{int}^{\ddagger}$). The lower activation energy of **TS1** originates from both a more favorable interaction energy ($\Delta E_{int}^{\ddagger} = -19.64$ kcal/mol for **TS1** *vs.* -17.52 kcal/mol for **TS3**) and a lower distortion energy ($\Delta E_{dist}^{\ddagger} = 33.01$ kcal/mol for **TS1** *vs.* 34.88 kcal/mol for **TS3**). Acetonitrile's linear structure is more rigid than acetone, and twisting requires more energy. A deeper decomposition of the interaction energy confirms the crucial role of electrostatics and orbital interactions. The electrostatic term ($\Delta E_{els}^{\ddagger}$) is significantly more stabilizing in **TS1** (-32.71 kcal/mol) than in **TS3** (-28.56 kcal/mol), providing robust quantitative support for the trend observed in the ESP analysis. Furthermore, the orbital interaction term ($\Delta E_{orb}^{\ddagger}$), which reflects the covalent character of the forming bond, is also substantially stronger in **TS1** (-11.95 kcal/mol) compared to **TS3** (-8.89 kcal/mol). Although $\Delta E_{xrep}^{\ddagger}$, which represents the steric hindrance effect, is higher in **TS1** (26.65 kcal/mol) compared to **TS3** (19.27 kcal/mol) because of acetone carries two methyl groups with larger steric hindrance, which strongly repel the substrate fragment in the transition state, thus it still exhibits stronger electrostatic attraction and orbital interactions.

3. Conclusions

In conclusion, we propose a universal, convenient and green electrochemical synthesis approach for the [3 + 2] ring expansion of epoxides to yield 1,3-dioxolane, oxazoline and cyclic carbonate derivatives via the insertion of acetone, acetonitrile or carbon dioxide molecule. These reaction processes can be significantly promoted by employing Lewis-acidic ionic liquid supporting electrolytes and designed cathodic metal electrocatalysts (e.g., Pt and Rh) on carbon fibers. This approach offers mild reaction conditions, high efficiency, high atomic economy, ease of operation, and versatility for the mass production of five-membered heterocycle derivatives. Theoretical calculations support the preference for a concerted ring-expanding reaction pathway over a stepwise one in terms of kinetic favorability. The disparity in activation energy barriers for the rate-determining steps derived from different electrostatic attractions are visualized by the electrostatic potential surfaces, providing a reasonable explanation on the rapider reaction rate of acetone compared to that of acetonitrile. With the growing significance in the controllable synthesis of diversified oxygen- and/or nitrogen-containing heterocyclic compounds, and the notable merits of electrochemically driven reactions in green synthetic chemistry, this study presents an effective synthetic strategy for exploring this intriguing research domain.

CRediT authorship contribution statement

Qianchuan Yu: Formal analysis. **Huaizhu Wang:** Formal analysis. **Tianyu Shen:** Formal analysis. **Yizhi Xing:** Formal analysis. **Zuoxiu Tie:** Project administration. **Xingkai Ma:** Formal analysis. **Guochun Ding:** Formal analysis. **Zhong Jin:** Writing – review & editing, Writing – original draft, Supervision, Resources, Project administration, Funding acquisition, Conceptualization. **Yulong Fu:** Writing – original draft, Formal analysis, Data curation. **Pengbo Zhang:** Formal analysis. **Guoqiang Wang:** Writing – original draft, Software, Methodology, Formal analysis, Data curation. **Miao Wang:** Writing – review & editing, Writing – original draft, Validation, Formal analysis, Data curation, Conceptualization. **Shuhua Li:** Writing – original draft, Software, Resources, Formal analysis, Data curation. **Zuoao Wu:** Writing – original draft, Formal analysis, Data curation.

Declaration of Competing Interest

We declare that we do not have any commercial or associative interest that represents a conflict of interest in connection with the work submitted.

Acknowledgments

This work was supported by the National Natural Science Foundation of China (22479074, 22475096), the Equipment Pre-Research and Ministry of Education Joint Fund (8091B02052407), the Fundamental Research Program Key Project of Jiangsu Province (BK20253008), the Natural Science Foundation of Jiangsu Province (BK20240400, BK20241236), the Science and Technology Major Project of Jiangsu Province (BG2024013), the Scientific and Technological Achievements Transformation Special Fund of Jiangsu Province (BA2023037), the Academic Degree and Postgraduate Education Reforming Project of Jiangsu Province (JGKT24_C001), the Key Core Technology Open Competition Project of Suzhou City (SYG2024122), the Open Research Fund of Suzhou Laboratory (SZLAB-1308-2024-TS005), and the Chenzhou National Sustainable Development Agenda Innovation Demonstration Zone Provincial Special Project (No. 2023sfq11).

Supplementary materials

Experimental section; Materials and products characterizations; Computational details; Supplementary text; Fig. S1–S45; Table S1; XRD patterns; XPS spectra; SEM and elemental mapping images; TEM; V-t curves; Screening results of cathodic electrocatalysts; MS results; EIS; CV

curves; HPLC plots; ^{1}H and ^{13}C NMR spectra; FT-IR spectra; Scale-up experiment details; Electrochemical ring expansion of epoxide with carbon dioxide.

Appendix A. Supporting information

Supplementary data associated with this article can be found in the online version at doi:10.1016/j.nanoen.2025.111485.

Data availability

Data will be made available on request.

References

[1] M.H. Qureshi. The Njarðarson Group, The University of Arizona, Top 200 small molecule drugs by retail sales in 2022, 2022.
[2] V.G. Chandrashekhar, W. Baumann, M. Beller, R.V. Jagadeesh, Nickel-catalyzed hydrogenative coupling of nitriles and amines for general amine synthesis, Science 376 (2022) 1433–1441.
[3] E. Vitaku, D.T. Smith, J.T. Njardarson, Analysis of the structural diversity, substitution patterns, and frequency of nitrogen heterocycles among U.S. Fda approved pharmaceuticals: miniperspective, J. Med. Chem. 57 (2014) 10257–10274.
[4] R.D. Taylor, M. MacCoss, A.D.G. Lawson, Rings in drugs: miniperspective, J. Med. Chem. 57 (2014) 5845–5859.
[5] S.-M. Guo, S. Huh, M. Coehlo, L. Shen, G. Pieters, O. Baudoin, A C–H activation-based enantioselective synthesis of lower carbo[n]helicenes, Nat. Chem. 15 (2023) 872–880.
[6] W. Lee, Y. Koo, H. Jung, S. Chang, S. Hong, Energy-transfer-induced [3+2] cycloadditions of N–N pyridinium ylides, Nat. Chem. 15 (2023) 1091–1099.
[7] M. Mato, D. Spinnato, M. Leutzsch, H.W. Moon, E.J. Reijerse, J. Cornella, Bismuth radical catalysis in the activation and coupling of redox-active electrophiles, Nat. Chem. 15 (2023) 1138–1145.
[8] Y. Xiong, B. Li, Y. Gu, T. Yan, Z. Ni, S. Li, J.-L. Zuo, J. Ma, Z. Jin, Photocatalytic nitrogen fixation under an ambient atmosphere using a porous coordination polymer with bridging dinitrogen anions, Nat. Chem. 15 (2023) 286–293.
[9] R. Mykura, R. Sánchez-Bento, E. Matador, V.K. Duong, A. Varela, L. Angelini, R. J. Carbajo, J. Llaveria, A. Ruffoni, D. Leonori, Synthesis of polysubstituted azepanes by dearomative ring expansion of nitroarenes, Nat. Chem. 16 (2024) 771–779.
[10] K. Wang, L. Yang, Y. Li, H. Li, Z. Liu, L. Ning, X. Liu, X. Feng, Asymmetric catalytic ring-expansion of 3-methyleneazetidines with α-diazo pyrazoamides towards proline-derivatives, Angew. Chem. Int. Ed. 62 (2023) e202307249.
[11] E.E. Hyland, P.Q. Kelly, A.M. McKillop, B.D. Dherange, M.D. Levin, Unified access to pyrimidines and quinazolines enabled by n–n cleaving carbon atom insertion, J. Am. Chem. Soc. 144 (2022) 19258–19264.
[12] Z. Wang, L. Jiang, P. Sarró, M.G. Suero, Catalytic cleavage of $C(sp_2)$–$C(sp_2)$ bonds with Rh-carbynoids, J. Am. Chem. Soc. 141 (2019) 15509–15514.
[13] L. Chen, L.-N. Guo, S. Liu, L. Liu, X.-H. Duan, Visible-light-driven palladium-catalyzed Dowd–Beckwith ring expansion/C–C bond formation cascade, Chem. Sci. 12 (2021) 1791–1795.
[14] J.C. Reisenbauer, O. Green, A. Franchino, P. Finkelstein, B. Morandi, Late-stage diversification of indole skeletons through nitrogen atom insertion, Science 377 (2022) 1104–1109.
[15] J. Wang, H. Lu, Y. He, C. Jing, H. Wei, Cobalt-catalyzed nitrogen atom insertion in arylcycloalkenes, J. Am. Chem. Soc. 144 (2022) 22433–22439.
[16] Z. Siddiqi, W.C. Wertjes, D. Sarlah, Chemical equivalent of arene monooxygenases: dearomative synthesis of arene oxides and oxepines, J. Am. Chem. Soc. 142 (2020) 10125–10131.
[17] H. Lyu, I. Kevlishvili, X. Yu, P. Liu, G. Dong, Boron insertion into alkyl ether bonds via zinc/nickel tandem catalysis, Science 372 (2021) 175–182.
[18] R. Li, B. Li, H. Zhang, C.-W. Ju, Y. Qin, X.-S. Xue, D. Zhao, A ring expansion strategy towards diverse azaheterocycles, Nat. Chem. 13 (2021) 1006–1016.
[19] H. Wang, H. Shao, A. Das, S. Dutta, H.T. Chan, C. Daniliuc, K.N. Houk, F. Glorius, Dearomative ring expansion of thiophenes by bicyclobutane insertion, Science 381 (2023) 75–81.
[20] J.R.L. Smith, R.O.C. Norman, M.R. Stillings, Synthesis of oxazolines from epoxides, J. Chem. Soc. Perkin Trans. 1 (1975) 1200–1202.
[21] R. Ballini, G. Bosica, B. Frullanti, R. Maggi, G. Sartori, F. Schroer, 1,3-Dioxolanes from carbonyl compounds over zeolite HSZ-360 as a reusable, heterogeneous catalyst, Tetrahedron Lett. 39 (1998) 1615–1618.
[22] T. Takeda, S. Yasuhara, S. Watanabe, Preparation of 1,3-dioxolanes from epoxides and carbonyl compounds under neutral conditions, J. Jpn. Oil Chem. Soc. 30 (1981) 468–490.
[23] S.-H. Lee, J.-C. Lee, M.-X. Li, N.-S. Kim, Copper(II)-catalyzed formation of 1,3-dioxolanes from oxiranes, Bull. Korean Chem. Soc. 26 (2005) 221–222.
[24] F. Benfatti, G. Cardillo, L. Gentilucci, A. Tolomelli, M. Monari, F. Piccinelli, A microwave-enhanced, lewis acid-catalyzed synthesis of 1,3-dioxolanes and oxazolines from epoxides, Adv. Synth. Catal. 349 (2007) 1256–1264.
[25] Y. Hioki, M. Costantini, J. Griffin, K.C. Harper, M.P. Merini, B. Nissl, Y. Kawamata, P.S. Baran, Overcoming the limitations of kolbe coupling with waveform-controlled electrosynthesis, Science 380 (2023) 81–87.
[26] B. Zhang, J. He, Y. Gao, L. Levy, M.S. Oderinde, M.D. Palkowitz, T.G.M. Dhar, M. D. Mandler, M.R. Collins, D.C. Schmitt, P.N. Bolduc, T. Chen, S. Clementson, N. N. Petersen, G. Laudadio, C. Bi, Y. Kawamata, P.S. Baran, Complex molecule synthesis by electrocatalytic decarboxylative cross-coupling, Nature 623 (2023) 745–751.
[27] S. Gnaim, A. Bauer, H.-J. Zhang, L. Chen, C. Gannett, C.A. Malapit, D.E. Hill, D. Vogt, T. Tang, R.A. Daley, W. Hao, R. Zeng, M. Quertenmont, W.D. Beck, E. Kandahari, J.C. Vantourout, P.-G. Echeverria, H.D. Abruna, D.G. Blackmond, S. D. Minteer, S.E. Reisman, M.S. Sigman, P.S. Baran, Cobalt-electrocatalytic HAT for functionalization of unsaturated C–C bonds, Nature 605 (2022) 687–695.
[28] B. Zhang, Y. Gao, Y. Hioki, M.S. Oderinde, J.X. Qiao, K.X. Rodriguez, H.-J. Zhang, Y. Kawamata, P.S. Baran, Ni-electrocatalytic Csp_3–Csp_3 doubly decarboxylative coupling, Nature 606 (2022) 313–318.
[29] T. Peng, T. Zhuang, Y. Yan, J. Qian, G.R. Dick, J. Behaghel De Bueren, S.-F. Hung, Y. Zhang, Z. Wang, J. Wicks, F.P. Garcia De Arquer, J. Abed, N. Wang, A. Sedighian Rasouli, G. Lee, M. Wang, D. He, Z. Wang, Z. Liang, L. Song, X. Wang, B. Chen, A. Ozden, Y. Lum, W.R. Leow, M. Luo, D.M. Meira, A.H. Ip, J.S. Luterbacher, W. Zhao, E.H. Sargent, Ternary alloys enable efficient production of methoxylated chemicals via selective electrocatalytic hydrogenation of lignin monomers, J. Am. Chem. Soc. 143 (2021) 17226–17235.
[30] Y. Yao, Z. Huang, P. Xie, S.D. Lacey, R.J. Jacob, H. Xie, F. Chen, A. Nie, T. Pu, M. Rehwoldt, D. Yu, M.R. Zachariah, C. Wang, R. Shahbazian-Yassar, J. Li, L. Hu, Carbothermal shock synthesis of high-entropy-alloy nanoparticles, Science 359 (2018) 1489–1494.
[31] T. Li, Q. Dong, Z. Huang, L. Wu, Y. Yao, J. Gao, X. Wang, H. Zhang, D. Wang, T. Li, R. Shahbazian-Yassar, L. Hu, Interface engineering between Multi-Elemental alloy nanoparticles and a carbon support toward stable catalysts, Adv. Mater. 34 (2022) 2106436.
[32] S. Song, X. Li, J. Wei, W. Wang, Y. Zhang, L. Ai, Y. Zhu, X. Shi, X. Zhang, N. Jiao, DMSO-catalysed late-stage chlorination of (hetero)arenes, Nat. Catal. 3 (2019) 107–115.
[33] C. Li, Z. Yan, B. Wang, J. Li, W. Lyu, Z. Wang, N. Jiao, S. Song, Regioselective synthesis of 4-functionalized pyridines, Chem 10 (2024) 628–643.
[34] G.-Q. Sun, W. Zhang, L.-L. Liao, L. Li, Z.-H. Nie, J.-G. Wu, Z. Zhang, D.-G. Yu, Nickel-catalyzed electrochemical carboxylation of unactivated aryl and alkyl halides with CO_2, Nat. Commun. 12 (2021) 7086.
[35] C. Chen, X. Zhu, X. Wen, Y. Zhou, L. Zhou, H. Li, L. Tao, Q. Li, S. Du, T. Liu, D. Yan, C. Xie, Y. Zou, Y. Wang, R. Chen, J. Huo, Y. Li, J. Cheng, H. Su, X. Zhao, W. Cheng, Q. Liu, H. Lin, J. Luo, J. Chen, M. Dong, K. Cheng, C. Li, S. Wang, Coupling N_2 and CO_2 in H_2O to synthesize urea under ambient conditions, Nat. Chem. 12 (2020) 717–724.
[36] Y. Luo, K. Xie, P. Ou, C. Lavallais, T. Peng, Z. Chen, Z. Zhang, N. Wang, X.-Y. Li, I. Grigioni, B. Liu, D. Sinton, J.B. Dunn, E.H. Sargent, Selective electrochemical synthesis of urea from nitrate and CO_2 via relay catalysis on hybrid catalysts, Nat. Catal. 6 (2023) 939–948.
[37] Y. Fang, X. Liu, Z. Liu, L. Han, J. Ai, G. Zhao, O. Terasaki, C. Cui, J. Yang, C. Liu, Z. Zhou, L. Chen, S. Che, Synthesis of amino acids by electrocatalytic reduction of CO_2 on chiral Cu surfaces, Chem 9 (2023) 460–471.
[38] L. Li, W. Liu, R. Chen, S. Shang, X. Zhang, H. Wang, H. Zhang, B. Ye, Y. Xie, Atom-Economical synthesis of dimethyl carbonate from CO_2: engineering reactive frustrated lewis pairs on ceria with vacancy clusters, Angew. Chem. Int. Ed. 61 (2022) e202214490.
[39] L. Li, H. Ying, P. Qiao, W. Liu, S. Shang, W. Shao, H. Wang, X. Zhang, Y. Xie, Symmetry-Broken steered delocalization state in a Single-Atom photocatalyst, Nano Lett. 24 (2024) 14412–14420.
[40] L. Li, W. Liu, H. Ying, X. He, S. Shang, P. Zhang, X. Zhang, S. Liu, H. Wang, Y. Xie, Artificial Chlorophyll-like structure for photocatalytic CO_2 chemical fixation, CCS Chem. 6 (2024) 3077–3089.
[41] H. Khoshro, H.R. Zare, M. Namazian, A.A. Jafari, A. Gorji, Synthesis of cyclic carbonates through cycloaddition of electrocatalytic activated CO_2 to epoxides under mild conditions, Electrochim. Acta 113 (2013) 263–268.
[42] Y. Zhao, N.E. Schultz, D.G. Truhlar, Design of density functionals by combining the method of constraint satisfaction with parametrization for thermochemistry, thermochemical kinetics, and noncovalent interactions, J. Chem. Theory Comput. 2 (2006) 364–382.
[43] Y. Zhao, D.G. Truhlar, A new local density functional for main-group thermochemistry, transition metal bonding, thermochemical kinetics, and noncovalent interactions, J. Chem. Phys. 125 (2006) 194101.
[44] Y. Zhao, D.G. Truhlar, Density functional for spectroscopy: no long-range self-interaction error, good performance for rydberg and charge-transfer states, and better performance on average than B3LYP for ground states, J. Phys. Chem. A 110 (2006) 13126–13130.
[45] Y. Zhao, D.G. Truhlar, The M06 suite of density functionals for main group thermochemistry, thermochemical kinetics, noncovalent interactions, excited states, and transition elements: two new functionals and systematic testing of four M06-class functionals and 12 other functionals, Theor. Chem. Acc. 120 (2008) 215–241.
[46] M. Bortolami, L. Mattiello, V. Scarano, F. Vetica, M. Feroci, In situ anodically oxidized BMIm-BF_4: a safe and recyclable BF3 source, J. Org. Chem. 86 (2021) 16151–16157.
[47] T. Lu, F. Chen, Multiwfn: a multifunctional wavefunction analyzer, J. Comput. Chem. 33 (2012) 580–592.

[48] T. Lu, F. Chen, Quantitative analysis of molecular surface based on improved marching tetrahedra algorithm, J. Mol. Graph. Model 38 (2012) 314–323.
[49] J. Zhang, T. Lu, Efficient evaluation of electrostatic potential with computerized optimized code, Phys. Chem. Chem. Phys. 23 (2021) 20323–20328.
[50] T. Lu, Q. Chen, Simple, efficient, and universal energy decomposition analysis method based on dispersion-corrected density functional theory, J. Phys. Chem. A 127 (2023) 7023–7035.

Miao Wang received his Ph.D. degree in School of Chemistry and Materials Science from the University of Science and Technology of China (USTC) in 2019, and then worked as a postdoc (2019–2021) at Shenzhen University. Since 2021, he has served as associate research fellow under the supervision of Prof. Zhong Jin in School of Chemistry and Chemical Engineering at Nanjing University. His research focuses on the design of advanced functional crystal materials and devices for clean energy conversion and storage.

Zuoao Wu received his B.S. in applied chemistry from Sichuan University in 2020. He is currently pursuing his Ph.D. degree under the supervision of Prof. Zhong Jin in School of Chemistry and Chemical Engineering at Nanjing University. His research interests mainly focus on redox flow batteries and electrosynthesis.

Yulong Fu was born in Henan, China, in 2000. He received his Bachelor's degree from Nanjing University of Science and Technology in 2022. He commenced his Master's studies in 2022 under the supervision of Prof. Shuhua Li and Assoc. Prof. Guoqiang Wang at Nanjing University, focusing on machine learning applications in theoretical chemistry, transitioning to the PhD program in 2024 to pursue machine learning-assisted studies of transition metal complexes under the joint supervision of Prof. Jin Xie and Assoc. Prof. Jie Han at Nanjing University.

Pengbo Zhang received his PhD (2025) in chemistry from Nanjing University, P. R. China, under the supervision of Prof. Zhong Jin. His research interests primarily focus on large-scale, low-cost aqueous secondary batteries (aqueous organic flow batteries and multivalent-ion batteries), including electrochemical reversible molecular design, regulation mechanisms underlying the energy storage processes.

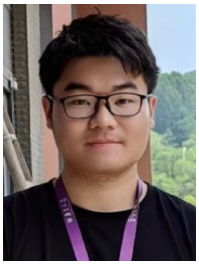

Huaizhu Wang received his B.S. degree in Chemistry from Nanjing University in 2021. He is now pursuing his Ph.D. degree under the supervision of Prof. Zhong Jin in School of Chemistry and Chemical Engineering, Nanjing University, P.R. China. His main interest is the efficient electrochemical synthesis of organic compounds.

Tianyu Shen received his PhD (2025) in chemistry from Nanjing University, P. R. China, under the supervision of Prof. Zhong Jin. His research interests primarily focus on design and development of energy storage devices (lithium batteries and zinc batteries), including the design and synthesis of electrode materials, optimization of electrolytes and gel electrolytes.

Yu Qianchuan has been pursuing a Ph.D. in Physical Chemistry at Nanjing University's School of Chemistry and Chemical Engineering since September 2021, under the supervision of Professor Jin Zhong. His current research focuses on the design and application of organic cathode materials for secondary batteries, including alkali and multivalent metal batteries.

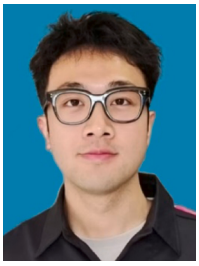

Xingkai Ma obtained his Ph.D. from the School of Chemistry and Chemical Engineering at Nanjing University. His research centers on organic electrode materials for new energy storage devices. He specializes in the chemical design, synthesis, and characterization of novel organic compounds for high-performance batteries, aiming to enhance energy density, power density, and cycle life through molecular engineering.

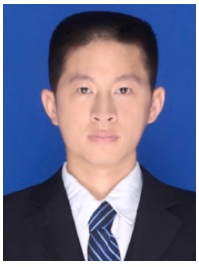

Guochun Ding received his MS Degree from the School of Chemistry and Chemical Engineering, Henan University of Technology in 2021, and he is now a doctoral candidate at the School of Chemistry and Chemical Engineering, Nanjing University under the supervision of Prof. Zhong Jin. His current research interests mainly focus on designing and synthesizing functional organic materials as electro-active species for aqueous redox flow batteries.

Yizhi Xing received his M.S. degree from the School of Chemical Engineering and Technology, Tianjin University, in 2022. He is currently a doctoral candidate at the School of Chemistry and Chemical Engineering, Nanjing University, under the supervision of Prof. Zhong Jin. His research focuses on safe aqueous batteries for large-scale energy storage, including electrolyte optimization for aqueous zinc batteries and the design and verification of novel aqueous battery systems.

Zuoxiu Tie received her BS (2004) and PhD (2009) in Physics from Nanjing University, P. R. China. Now she is a technician in the College of Engineer and Applied Sciences, Nanjing University. Her research focuses on the development of next-generation energy materials.

Guoqiang Wang received his PhD in chemistry from Nanjing University, China, in 2016. He worked as a postdoctoral researcher at the School of Physics of Nanjing University (2016–2020) and at the Technical University of Berlin, Germany (2019–2020). Since 2021, he has been an associate professor at Nanjing University. His research focuses on computation and data-driven reaction design, as well as AI-assisted chemical synthesis.

Shuhua Li received his PhD in chemistry from Nanjing University, China, in 1996. He worked as a postdoctoral researcher at the Department of Physics of Nanjing University (1996–1998) and at the Department of Chemistry of Texas A&M University, USA (1998–2000). Since 2002, he has been a professor at the School of Chemistry and Chemical Engineering of Nanjing University. His research interests focus on the development and application of quantum chemical methods for complex chemical systems.

Zhong Jin received his BS (2003) and PhD (2008) in chemistry from Peking University, P. R. China. He worked as a postdoctoral scholar at Rice University (2008–2010) and Massachusetts Institute of Technology (2010–2014). Now he is a professor and the Director of the Institute of Green Chemistry and Engineering at Nanjing University. He leads a research group working on functional nanomaterials and devices for clean energy conversion and storage applications.